Nano-scale modeling and elastic properties of a typical C-SH (I) structure based on Density Functional Theory and Molecular Dynamics Methods

Jia Fu[1]*, Fabrice Bernard[2], Siham Kamali-Bernard[3], Weihui Lin[4]

[1] *LGCGM, INSA de Rennes, 35708; School of Material Science and Engineering, Northwestern Polytechnical University, Xi'an 710072, Jia.Fu@insa-rennes.fr.*

[2] *LGCGM, INSA de Rennes, 35708, Fabrice.Bernard@insa-rennes.fr.*

[3] *LGCGM, INSA de Rennes, 35708, siham.kamali-bernard@insa-rennes.fr.*

[4] *Mechanics College, Taiyuan University of Technology, Taiyuan 030024, lwhtyut@163.com.*

RÉSUMÉ. Les silicates de calcium hydratés (C-S-H) sont les constituants principaux de la pâte de ciment et ont donc une grande influence sur les propriétés mécaniques des matériaux cimentaires. Le modèle de tobermorite-11Å (formule chimique: $Ca_4Si_6O_{14}(OH)_4{\cdot}2H_2O$) est d'abord considéré comme configuration initiale pour décrire ces hydrates. Ce modèle est alors étudié par DFT (Density Functional Theory) et Dynamique Moléculaire. Les constantes élastiques sont calculées et comparées à des valeurs expérimentales. Un Silicate de Calcium Hydraté amorphe est obtenu par le biais d'une modélisation par Dynamique Moléculaire d'un processus de recuit de la tobermorite-11Å avec utilisation d'un potentiel de Born-Huggins-Meyer (BMH). Des tests uniaxiaux de traction et de compression d'un silicate de calcium hydraté amorphe (avec un rapport Ca/Si de 0,67), à une certaine vitesse de déformation, sont modélisés. Les courbes contrainte-déformation sont analysées. Les résultats montrent que: (1) les coefficients élastiques C_{ij} dans la plage de pression de confinement 0~1GPa sont obtenus pour vérifier la fiabilité du modèle de monocristal de 11Å tobermorite par comparaison avec des résultats de la littérature obtenus pour 0 GPa de confinement. (2) Un modèle de super-cellule à l'échelle nano montre des propriétés mécaniques isotropes. (3) Après recuit pour obtenir un C-S-H (I) amorphe, le module de Young est en moyenne d'environ 21,41 GPa.

ABSTRACT. C-S-H is the most important binding phase of cement paste and thus has a great influence on the mechanical properties of cement-based materials. The 11Å tobermorite model (chemical formula: $Ca_4Si_6O_{14}(OH)_4{\cdot}2H_2O$) as a initial configuration is established first, and then studied by DFT (Density Functional Theory) and Molecular Dynamics. Elastic constants are calculated with comparison with experimental ones and then a represented amorphous hydrated calcium silicate-11Å tobermorite, obtained by Molecular Dynamics, based on Born-Huggins-Meyer (BMH) potential is proposed. Finally, the stretch and compression process of a represented amorphous hydrated calcium silicate (Ca/Si ratio is 0.67) at a certain strain rate are calculated and the corresponding tensile and compressive stress-strain curves are analyzed. The results show that: (1) Elastic coefficient variation C_{ij} within 0~1Gpa pressure range is obtained to check the reliability of the single crystal model of 11Å tobermorite with the experimental comparison at 0GPa. (2) A supercell model at nano-scale shows the isotropy of the C-S-H phase for low strain rate. (3) After annealing to obtain amorphous C-S-H (I), Young's modulus in z-direction is averaged to be about 21.41 GPa.

MOTS-CLÉS : Echelle nanométrique, Tobermorite, Dynamique moléculaire, DFT, Élasticité anisotrope, Module d'Young.

KEY WORDS: Nanoscale, Tobermorite, Molecular dynamics, DFT, Anisotropic elasticity, Yong's module.

1. Introduction

Cement is the most widely used construction material in the world. The cement powder contains more particularly two calcium silicates Ca_2SiO_4 and Ca_3SiO_5 (respectively C_2S and C_3S in the cement manufacture notations). These two anhydrous components account for more than two thirds of the Portland cement weight and they lead, after hydration, to synthetic products named Calcium Silicates Hydrates (C-S-H). The chemical composition of these hydrates is variable. In particular, their structural Ca/Si ratio varies from 0.6 to 2.3 with eventually spatial heterogeneity within a given cement paste [RIC 93]. In neat Portland cement, only the C-S-H with the highest Ca/Si ratio (>~1.5) are observed, whereas C-S-H with the whole compositional range may exist in cement pastes containing fly ash, metakaolin or silica fume [GIR 10, PLA 04].

The C-S-H phase is often called C-S-H gel since it is described as an amorphous phase with no long-range order. Short and medium-range order in C-S-H has therefore been extensively investigated with a variety of physical methods, such as transmission electron microscopy [GRO 86], Fourier-transform infrared [YU 99], Raman spectroscopy [KIR 97] or X-ray absorption fine structure spectroscopy (EXAFS) [LEQ 99]… A partially ordered layer stacking may be put into evidence. Following the earliest works of Taylor and Howison [Taylor et al., 1956], it has been found that when the Ca/Si ratio matches that of tobermorite, C-S-H structure is thought to be close to this model mineral [GRA 13]. In the literature, three main varieties of tobermorite have been differentiated from their layer-to-layer distance (9Å, 11Å or 14Å). C-S-H has a great influence on the mechanical properties of the cement paste and it is the most important binding phase of cement paste. Also C-S-H is a typical constituent of the micro-scale Portland Hydrated Cement Paste (HPCP) (KAM 09) and its Young's modulus is needed in a 3D multi-scale mortar model (BER 08). The assessment of the mechanical properties of this binding phase is of undeniable practical importance. It is now well recognized that such an objective can be achieved by means of linking the structure of the phase at the atomic scale with its performance. The development of modelling tools is thus anavoidable. Nano-scale modelling methods mainly include molecular structural mechanics method (MSMM), molecular dynamics (MD), the ab-initio calculation, tight-binding (TB) and the density functional theory (DFT).

In recent years, some scholars have successfully simulated C-S-H structure by MD simulations.Pellenq and co-workers [PEL 08] have simulated several tobermorite structures by using the General Utility Lattice Program (GULP), where GULP uses the core-shell potential. Kalinichev and co-workers [KAL 07] have simulated the tobermorite structure using ClayFF force field [CYG 04], where water molecules are modelled using Simple Point Charge (SPC) model, and it is indicated that the water shows very strong binding force in the solid surface. Pellenq and co-workers [PEL 09] have developed a new modeling method to simulate C-S-H gel structure, of which it has a shorter $[SiO_4]^{4-}$ chain under the system equilibrium structure $C_{1.65}$-S-$H_{1.75}$, comparing with experimental values of $C_{1.7}$-S-$H_{1.8}$ [ALL 09]. Shahsavari and co-workers [SHA 11] proposed a new CSH-FF Field with a higher accuracy and more efficient than the traditional core-shell potential. Ji and co-workers [JI 12] have simulated the influencing role of a variety of water molecules (usually optional SPC model) on C-S-H by using GROMACS [BER 95] program, mainly used a simple harmonic force potential description of C-S-H between atoms and ions. Zaoui [ZAO 12] has simulated tobermorite structure of different Ca/Si ratios under various pressures, of which Buckingham potential [SCH 92] and core-shell potential are used. This author found that the elastic modulus of different Ca/Si ratio tobermorite structures tends to be similar with increasing pressure. Some scholars [ZHA 05] develop the DL_POLY program to simulate the tobermorite by MD, finding that amorphous form of C-S-H (I) is a short-range structure and long-range disordered structure, which is more consistent with the experimental parameters. Dai Wei [DAI 12] has compared two C-S-H structures of different Ca/Si ratios and discussed MD modelling parameters, of which the COMPASS force field is mainly used.

In this work, the 11Å tobermorite model (chemical formula: $Ca_4Si_6O_{14}(OH)_4{\cdot}2H_2O$) as a initial configuration is established first, and then calculated by LAMMPS program after setting parameters of related potential function. Elastic constants are calculated with comparison of experimental ones and then a represented amorphous hydrated calcium silicate-11Å tobermorite based on Born-Huggins-Meyer (BMH) potential is proposed. Finally, the stretch and compression process of a represented amorphous hydrated calcium silicate (the ratio of Ca/Si is 0.67) at a certain strain rate are calculated and the corresponding tensile and compressive stress-strain curves are analyzed.

2. C-S-H interatomic potential type and elastic modulus determination

2.1. Interatomic potentials of C-S-H

The multi-body potential of crystal structure can be defined by different interatomic potentials by Brahim Khalil Benazzouz [BEN 10]. The potential energy of C-S-H structure can be computed by summing the energy

from different types of interactions that occur in a system (i.e., two-body and three-body interactions) [MUR 07]. Thus we can use Buckingham or Born-Huggins-Meyer (BMH) potential for short-range term, Stillinger–Weber (three boy potential of long-range term) and Coulomb potentials to describe atomic interactions.

So for C-S-H structure, the born style computes the Born-Mayer-Huggins or Tosi/Fumi potential described in [FUM 64], given by:

$$U_{ij}^{BMH} = A\exp\left(\frac{\sigma - r}{\rho}\right) - \frac{C}{r^6} + \frac{D}{r^8} \quad (r < r_c) \qquad [1]$$

Where σ is an interaction-dependent length parameter, r is an ionic-pair dependent length parameter, and r_c is the cutoff length.

Interactions between two atoms can be processed through the standard Buckingham potential to describe the interactions of two atoms and the Coulomb term, the expression is as follows:

$$U_{ij}^{Buckingham} = A\exp\left(-\frac{r_{ij}}{\rho}\right) - \frac{C}{r_{ij}^6} + \frac{q_i q_j}{4\pi\varepsilon_0 r_{ij}} \qquad [2]$$

Where, r_{ij} is the length of the link between two atoms i and j, q_i is the charge of the ion i and ε_0 is the electron charge.

For Stillinger–Weber potential to describe the interaction between O-Si-O bonds, parameters can be obtained by S.J.Murray [MUR 07]. The corresponding values of the parameters of A, ρ and C are shown in Tab.1.

2.2. Relationship between Young's modulus and elastic constants

Stress-strain relation in an orthotropic monoclinic crystal can be defined by the independent elastic stiffness parameters [WU 07]:

$$\begin{bmatrix} \sigma_{11} \\ \sigma_{22} \\ \sigma_{33} \\ \sigma_{12} \\ \sigma_{13} \\ \sigma_{23} \end{bmatrix} = \begin{bmatrix} c_{11} & c_{12} & c_{13} & 0 & 0 & c_{16} \\ c_{12} & c_{22} & c_{23} & 0 & 0 & c_{26} \\ c_{13} & c_{23} & c_{33} & 0 & 0 & c_{36} \\ 0 & 0 & 0 & c_{44} & c_{45} & 0 \\ 0 & 0 & 0 & c_{45} & c_{55} & 0 \\ c_{16} & c_{26} & c_{36} & 0 & 0 & c_{66} \end{bmatrix} \begin{bmatrix} \varepsilon_{11} \\ \varepsilon_{22} \\ \varepsilon_{33} \\ \gamma_{12} \\ \gamma_{13} \\ \gamma_{23} \end{bmatrix} \qquad [3]$$

Where, σ represents the normal stress and shear stress in each direction (unit: nN/nm^2); ε and γ are the normal strain and shear strain in each direction.

For monoclinic crystal/structure, elastic constants include: C_{11}, C_{22}, C_{33}, C_{l2}, C_{13}, C_{23}, C_{44}, C_{55}, C_{66} C_{l5}, C_{25}, C_{35} and C_{46}. The criteria for mechanical stability are given by: $C_{11}>0$, $C_{22}>0$, $C_{33}>0$, $C_{44}>0$, $C_{55}>0$,$C_{66}>0$, $\left[c_{11}+c_{22}+c_{33}+2(c_{12}+c_{13}+c_{23})\right]>0$; $\left(c_{44}c_{66}-c_{46}^2\right)>0$; $\left(c_{22}+c_{33}-2c_{23}\right)>0$; $\left[c_{22}\left(c_{33}c_{55}-c_{35}^2\right)+2c_{23}c_{25}c_{35}-c_{23}^2c_{55}-c_{25}^2c_{33}\right]>0$; $\left(c_{33}c_{55}-c_{35}^2\right)>0$; $\left\{2\left[c_{15}c_{25}\left(c_{33}c_{12}-c_{13}c_{23}\right)+c_{15}c_{35}\left(c_{22}c_{13}-c_{12}c_{23}\right)+c_{25}c_{35}\left(c_{11}c_{23}-c_{12}c_{13}\right)\right]-\left[c_{15}^2\left(c_{22}c_{33}-c_{23}^2\right)+c_{25}^2\left(c_{11}c_{33}-c_{13}^2\right)+c_{35}^2\left(c_{11}c_{22}-c_{12}^2\right)\right]+gc_{55}\right\}>0$.

The homogenized elastic properties of polycrystals can be separately calculated based on Voigt (V) and Reuss (R) bounds, of which shear modulus and bulk modulus are as follows:

$$G_V = \frac{1}{15}\left[c_{11}+c_{22}+c_{33}+3\left(c_{44}+c_{55}+c_{66}\right)-\left(c_{12}+c_{13}+c_{23}\right)\right] \qquad [4]$$

$$\begin{aligned} G_R = 15\Big\{ & 4\Big[\left(c_{33}c_{55}-c_{35}^2\right)\left(c_{11}+c_{22}+c_{12}\right)+\left(c_{23}c_{55}-c_{25}c_{35}\right)\left(c_{11}-c_{12}-c_{23}\right)+\left(c_{13}c_{35}-c_{15}c_{33}\right)\left(c_{15}+c_{25}\right) \\ & +\left(c_{13}c_{55}-c_{15}c_{35}\right)\cdot\left(c_{22}-c_{12}-c_{23}-c_{13}\right)+\left(c_{13}c_{25}-c_{15}c_{23}\right)\left(c_{15}-c_{25}\right)+f\Big]/\Omega+3\Big[g/\Omega+\left(c_{44}+c_{66}\right)/\left(c_{44}c_{66}-c_{46}^2\right)\Big]\Big\}^{-1} \end{aligned} \qquad [5]$$

$$B_V = \left[c_{11}+c_{22}+c_{33}+2\left(c_{12}+c_{13}+c_{23}\right)\right]/9 \qquad [6]$$

$$\begin{aligned} B_R = \Omega\Big[& \left(c_{33}c_{55}-c_{35}^2\right)\left(c_{11}+c_{22}-2c_{12}\right)+\left(c_{23}c_{55}-c_{25}c_{35}\right)\left(2c_{12}-2c_{11}-c_{23}\right)+\left(c_{13}c_{35}-c_{15}c_{33}\right)\cdot \\ & \left(c_{15}-2c_{25}\right)+\left(c_{13}c_{55}-c_{15}c_{35}\right)\left(2c_{12}+2c_{23}-c_{13}-2c_{22}\right)+2\left(c_{13}c_{25}-c_{15}c_{23}\right)\left(c_{25}-c_{15}\right)+f\Big]^{-1} \end{aligned} \qquad [7]$$

$$f = c_{11}\left(c_{22}c_{55}-c_{25}^2\right)-c_{12}\left(c_{12}c_{55}-c_{15}c_{25}\right)+c_{15}\left(c_{12}c_{25}-c_{15}c_{22}\right)+c_{25}\left(c_{23}c_{35}-c_{25}c_{33}\right) \qquad [8]$$

$$g = c_{11}c_{22}c_{33}-c_{11}c_{23}^2-c_{22}c_{13}^2-c_{33}c_{12}^2+2c_{12}c_{13}c_{23} \qquad [9]$$

$$\Omega = 2\left[c_{15}c_{25}\left(c_{33}c_{12}-c_{13}c_{23}\right)+c_{15}c_{35}\left(c_{22}c_{13}-c_{12}c_{23}\right)+c_{25}c_{35}\left(c_{11}c_{23}-c_{12}c_{13}\right)\right] - \left[c_{15}^2\left(c_{22}c_{33}-c_{23}^2\right)+c_{25}^2\left(c_{11}c_{33}-c_{13}^2\right)+c_{35}^2\left(c_{11}c_{22}-c_{12}^2\right)\right]+gc_{55} \quad [10]$$

In terms of the Voigt-Reuss-Hill approximations [HIL 52] $M_H = (1/2)(M_R+M_V)$, $M=B, G$. Young's modulus E and Possion's ratio μ are obtained:

$$E = \frac{9BG}{3B+G} = \frac{9\left(B_V/2+B_R/2\right)\left(G_V/2+G_R/2\right)}{3\left(B_V/2+B_R/2\right)+\left(G_V/2+G_R/2\right)} \quad [11]$$

$$\mu = \frac{3B-2G}{2\left(3B+G\right)} = \frac{3\left(B_V/2+B_R/2\right)-2\left(G_V/2+G_R/2\right)}{6\left(B_V/2+B_R/2\right)+2\left(G_V/2+G_R/2\right)} \quad [12]$$

Then homogenized elastic properties of polycrystals can be calculated, of which shear, bulk and Young's moduli can be obtained by calculating Voigt and Reuss bounds and averaging term [WU 07].

3. Modelling of 11Å tobermorite and elastic constants calculation by DFT

Density functional theory is a kind of first-principles molecular dynamics calculations [CAR 85, KRE 96], it is also called ab initio molecular dynamics [CAR 85]. The main difference between first-principles molecular dynamics and classical molecular dynamics is to calculate the interaction force between atoms. First-principles molecular dynamics make up the classical molecular dynamics need to know the atomic interaction potential shortcomings. The atomic interaction potential is solved by the density functional theory [KRE 96], and then substituted into the equations of motion of the atoms to solve the trajectory of the particles in the system.

3.1. Morphology and modeling of 11 Å tobermorite

The morphology of 11Å tobermorite is monoclinic and the lattice is as: a=6.69 Å, b=7.39Å, c=22.77Å, $\alpha=\beta$=90°, γ=123.49°, its structure is monoclinic with space group P21 [HAM 81]. Modeling of 11Å tobermorite and MD calculation are shown in Figure 1.

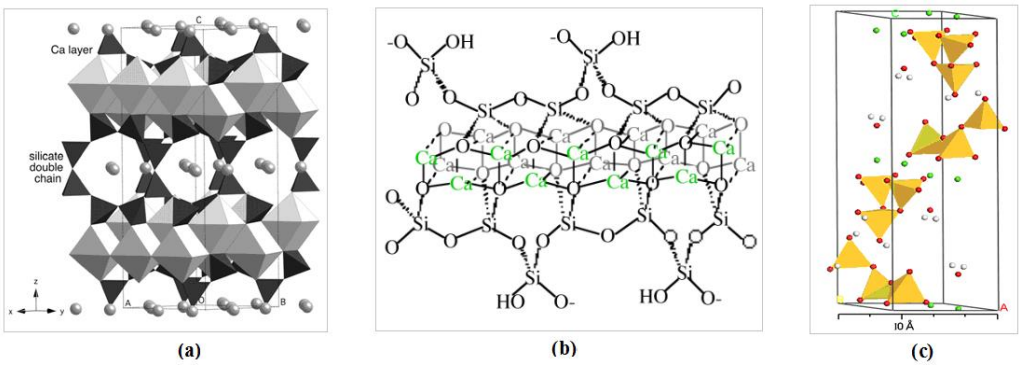

Figure 1. *Modeling of 11Å tobermorite: a) Structure of 11Å tobermorite; b) Silicon chain links and atomic connections; c) The real unit cell of 11Å tobermorite;*

In Figure 1 (a), the 11 Å tobermorite can be summarized as: (1) the structure is basically a layered structure with the central part is a Ca–O sheet (with an empirical formula: CaO2, of which the oxygen in CaO2 also includes that of the silicate tetrahedron part). (3) Silicate chains envelope the Ca–O sheet on both sides (shown in Figure 1 b). (4) Ca^{2+} and H_2O are filled between individual layers to balance the charges. The unit cell/crystal is shown in Figure 1(c), the infinite layers of calcium polyhedra which is parallel to (001), with tetrahedral chains of wollastonite-type along b and the composite layers stacked along c and connected through formation of double tetrahedral chains [MER 01].

3.2. Results of 11Å tobermorite model by DFT

In order to determine whether the elastic coefficients under various pressures are stable, the pressure region of 0-1GPa using DFT methods is added, with the initial conditions are as: the generalized gradient approximation is chosen and ultrasoft pseudopotentials cutoff energy of the plane waves is 400*eV*. Brillouin zone is *6×6×4*. Self-consistent convergence of the total energy per atom is chosen 10^{-4} *eV*. Elastic constants of CSH model based on DFT are calculated, shown in Figure 2 b), and then elastic modulus can be obtained [WU 07]. A comparison with previous results [SHA 09] is provided. Elastic constants of 11Å tobermorite monoclinic crystal under pressure 0～1.0GPa by DFT are in Figure 2.

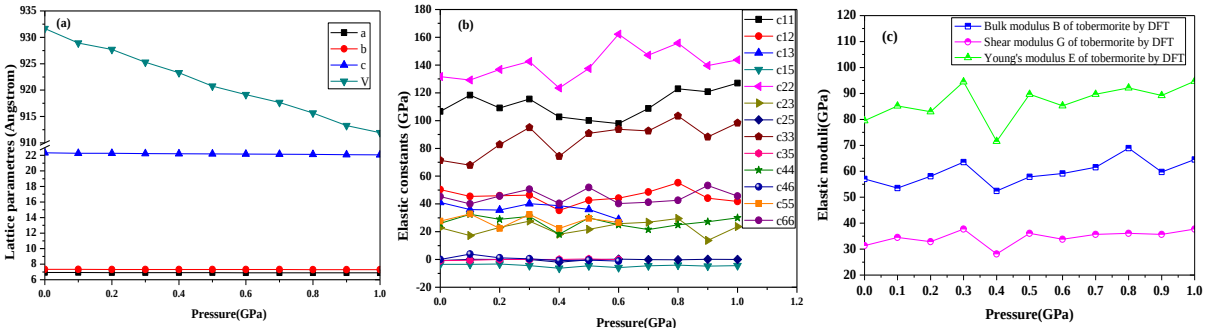

Figure 2. *11Å tobermorite crystal under pressure 0～1.0GPa: a) Change of a, c and V; b) Elastic constants. c) Elastic moduli.*

As shown in Fig.2 a), it can be seen that 11 Å tobermorite has not undergone a phase transition according to the smooth variation of lattice parameters *a*, *b*, *c* and cell volume *V* with the increase of pressure. Elastic constants by DFT are calculated in Figure 2 b), bulk modulus *B* (*GPa*), shear modulus *G* (*GPa*) are separately calculated by formula of equation (4)-(10), thus elastic moduli of C-S-H (I) are verified and averaged as *Gv*=32.815GPa; *Bv*=59.803GPa; *Gr*=29.908GPa; *Br*=54.276GPa; *E*=79.512GPa; μ=0.268 in Figure 2 c). Young's modulus of tobermorite is about 79.512GPa by Reuss-Voigt-Hill estimation, which is close to the simulation result of 89GPa [PEL 08] and result of 65GPa [SHA 09]. However, these simulation values by different modeling methods considering the ordered *Si* chain at long-range are far away from the experimental results of nanoindentation, performed on the C-S-H phase, available in the literature [VAN 13, MIL 08]. That confirms another time the absence of order at long-range in this phase and that the up-scalling to polycrystals cannot be done with the tobermorite model. This finding is agreement with results of [MAN 07].

4. Elastic properties of amorphous C-S-H (I) by MD method

4.1. Obtention of the amorphous structure and potential parameters

Based on crystal model of single 11Å tobermorite, a supercell (4a×3b×2c) of 11Å tobermorite model is established at nano-scale and then deformed, as shown in Figure 3.

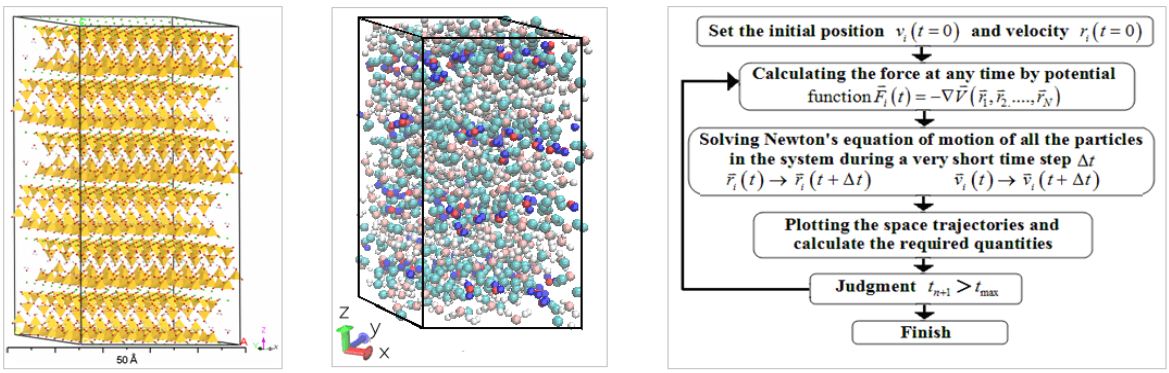

(a) **(b)** **(c)**

Figure 3. *Deformation of a supercell (4a×3b×2c) model during annealing processes based on MD: a) A* 2.676*nm*×2.217*nm*×4.554*nm model; b) The supercell structure in VDM software; c) Solving flowchart by MD.*

Based on the supercell (4a×3b×2c) model of 11Å tobermorite (in Figure 3 a), LAMMPS as a free molecular dynamics software is used and a corresponding code is developed to obtain the amorphous supercell structure by annealing treatment. The variables throughout the simulation are: the number of atoms *N*, the volume of simulation box *V*, the energy of the atoms *E* and the temperature of the atoms *T*. Initial supercell structure of C-S-H (I) in Visual Molecular Dynamics (VDM) software is shown in Figure 3 b). Steps of obtaining the annealed amorphous structure is as follows: 1) energy minimization by Conjugate Gradient (CG) method first, and then balance the structure in at 300*K* with10,000 steps separately under *NVT* and *NVE* system, and the time step is 0.1*fs* (femtosecond); 2) continue to balance the structure at a higher temperature of 3000*K* with 80000 steps under *NVT* and *NVE* system respectively, the time step is 1.0*fs*;3) change temperature from 3000*K* to 300*K* under *NVT* system and run 270 000 steps with the time step of 1.0*fs*; 4) Finally, the last turn is to balance the structure at 300*K* with 80 000 steps under *NVT* and *NVE* system by the time step 1*fs*, thus leads to an amorphous structure. Finally, the stretch and compression process of a represented amorphous C-S-H (I) at a certain strain rate are mainly calculated by the Born-Huggins-Meyer (BMH) potential and SPC water model [CYG 04], with

the solving flowchart by MD (Figure 3c). CSH parameters of Atomic Force Field employed are shown in Table 1.

Table 1. *CSH (I) parameters of Atomic Force Field employed (1e=1.6021892×10^{-19}C).*

Charges[SHA 11]		Born-Huggins-Meyer [FEU 90]			Buckingham [MUR 07]		
Species	charges [*e*]	bond	A_{ij}×10^{-11} /J	ρ_{ij} /nm	bond	A (*eV*)	ρ (*Å*)
Bridging oxygen Oss	-1.14	Si–Si	1.754	0.029	Si–Si	1171.52	0.29
Oxygen O	-1.14	Si–O	2.516	0.029	Si–O	1848.72	0.29
Silicon Si	1.72	O–O	0.372	0.029	O–O	452.51	0.29
Calcium Ca	1.42	Si–Ca	6.729	0.029	Si–Ca	1382.48	0.29
Oxygen (with H) Osh	-1.00	O–Ca	9.823	0.029	O–Ca	3557.62	0.29
Hydrogen Hos	0.29	Ca–Ca	25.582	0.029	Ca–Ca	4369.01	0.29
Water hydrogen Hw	0.41	Si–H	0.0644	0.029	Si–H	430.66	0.29
Water oxygen Ow	-0.82	H–H	0.0318	0.035	H–H	21.221	0.35
Interlayer calcium Cw	1.70	O–H	0.372	0.029	O–H	248.63	0.29

4.2. Simulation of uniaxial tests and influence of water molecules

Then the stretch and compression process of a represented amorphous hydrated calcium silicate (the ratio of Ca/Si is 0.67) at a certain strain rate (1×10^{-6}～1×10^{-3}) are calculated. Figure 4 shows the nano-structure evolution of the difference strain under the tensile strain rate of 1×10^{-4}.

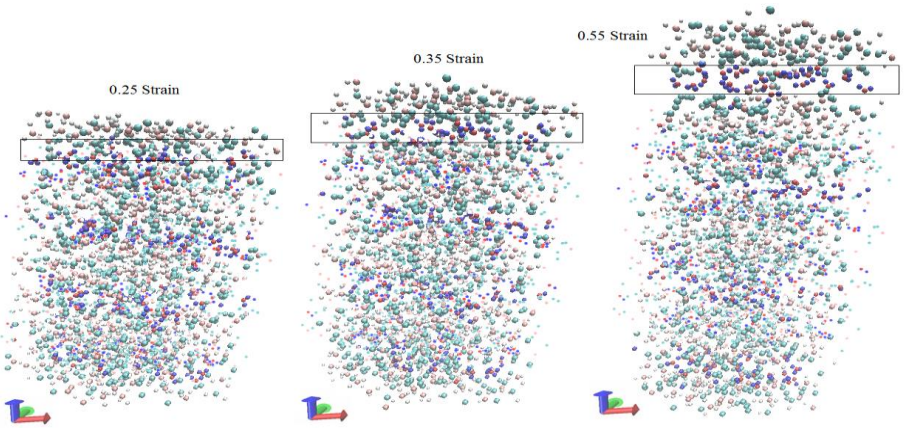

Figure 4: *Aggregation of water molecules during under difference strain with tensile strain rate of 1×10^{-4}*

From Figure 4, it is indicated that the water molecule has great impact on the mechanical properties of C-S-H (I) during tensile deformation. With increasing strain, the water molecules present in the places where an aqueous layer, and has a tendency to be pulled off in the intensive place of H_2O molecules, which may explain the cause of C-S-H (I) stress decrease during tensile process.

The stretch and compression process of an amorphous C-S-H (I) are calculated. The corresponding tensile and compressive stress-strain curves are in Figure 5.

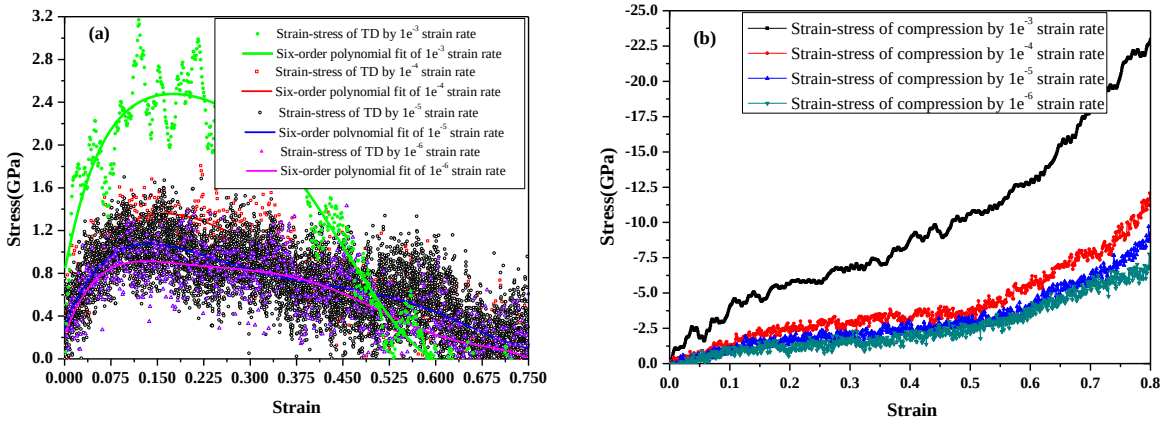

Figure 5: *a) Tensional stress-strain of a supercell structure after annealing by MD; b) Compressive stress-strain of a supercell structure after annealing by MD.*

As is shown in Figure 5a), the 4a×3b×2c supercell (2.676*nm*×2.217*nm*×4.554*nm*) of 11Å tobermorite after annealing is simulated (tensional strain rate 1.0×10^{-4}) by MD to obtain the amorphous structure and Young's module by fitting stress-strain curve is estimated about 18.562～24.298*GPa*, thus is averaged to be 21.43*GPa* by the different strain-stress slope. The expression of the interatomic bonds does not allow to predict the appearance of a peak in the compressive behavior. The simulations we conducted in Figure 5b) do not contradict this intuition but further work is needed to investigate this point.

After annealing treatment on Lammps, the ordered silicon chain becomes disordered and the system becomes more stable compared to the initial structure, which is consistent with the real structure of C-S-H (I). As a kind of LD C-S-H, 11Å tobermorite supercell becomes to the denser and more stable configuration after annealing (the initial C-S-H (I) structure after annealing has transferred from ordered structure to disordered structure), which is in agreement with the previously proposed quantitative "colloid" model of C-S-H gel, resulting in an improved understanding of the structural changes associated with drying and heat curing [JEN 07].

5. Conclusion

The stretch and compression process of a represented amorphous C-S-H (I) at a certain strain rate are calculated and the corresponding tensile and compressive stress-strain curves are analyzed. The results show that:

– Young's module of 11Å tobermorite is about 79.51GPa, according to elastic constants calculated by DFT.

– A supercell (4a×3b×2c) of 11Å tobermorite model at nano-scale shows the heterogeneous mechanical properties at three directions, of which z direction shows weakest loading resistance. After annealing process to obtain amorphous C-S-H (I), C-S-H (I) at nanoscale has a stronger compressive property but a weaker tensile property. Young's modulus in z directions is about 18.504～24.316GPa and is averaged to be about 21.43 GPa.

– Through annealing simulation, Young's modulus is significantly reduced, which is closer to the experimental value, indicating that the annealed supercell with disordered silicon chain is more realistic than the ordered silicon chain in practice.

– The water molecule in the structure has a great influence on tensile strength.

Acknowledgements: The authors acknowledge the financial support provided by China Scholarship Council (CSC) and support of state key laboratory of solidification processing, Northwestern Polytechnical University.

6. References

[ALL 07] A. J. ALLEN, J. J. THOMAS, H. M. JENNINGS, « Composition and density of nanoscale calcium-silicate-hydrate in cement », *Nature materials*, vol. 4, n° 6, 2007, p. 311-316.

[BEN 10] B.K. BENAZZOUZ, « Etude par dynamique moléculaire des propriétés mécaniques et thermodynamiques de l'argile de type kaolinite », Thèse de doctorat, l'université Lille Sciences et Technologies, 2010, France (in French).

[BER 95] H.J.C. BERENDSEN, D. VAN DER SPOEL, R. VAN DRUNEN, « GROMACS: a message-passing parallel molecular dynamics implementation », *Computer Physics Communications*, vol. 1-3, n° 91, 1995, p.43-56.

[BER 08] F. BERNARD, S. KAMALI-BERNARD, W. PRINCE. « 3D multi-scale modelling of mechanical behavior of sound and leached mortar », *Cement and Concrete Research*, vol. 38, 2008, p. 449–458.

[CAR 85] Car R, Parrinello M. « Unified approach for molecular dynamics and density-functional theory ». *Physical Review Letters*, vol. 22, n° 55, 1985, p. 2471–2474.

[CYG 04] R.T. CYGAN, J.J. LIANG, A.G. KALINICHEV, « Molecular models of hydroxide, oxyhydroxide, and clay phases and the development of a general force field », *Journal of Physical Chemistry B*, vol. 4 , n° 108, 2004,p. 1255-1266.

[DAI 12] W. DAI, Z. SHUI, P. DUAN. « Study on the Structural Model of Calcium Silicate Hydrate based on Computer Simulation », *2012 International Conference on Computer Technology and Science*, vol.47, 2012, p.1-5.

[FUM 64] F.G. FUMI AND M.P. TOSI, « Ionic sizes and Born repulsive parameters in the NaCl-type alkali halides: the Huggins-Mayer and Pauling forms », *Journal of Physics and Chemistry of Solids*, vol. 25, n° 45, 1964, p.31-44.

[FEU 90] B.P. FEUSTON, S.H. GAROFALINI, « Oligomerization in silica sols », *Journal Physical Chemistry*, vol. 13, n° 94, 1990, p.5351–5356.

[GIR 10] A.V. Girão, I.G. Richardson, R. Taylor, R.M.D. Brydson, « Composition, morphology and nanostructure of C-S-H in 70% white Portland cement–30% fly ash blends hydrated at 55 °C », *Cement and Concrete Research*, vol. 40 , 2010, p. 1350–1359.

[GRA 13] Sylvain Grangeon, Francis Claret, Catherine Lerouge, Fabienne Warmont, Tsutomu Sato, Sohtaro Anraku, Chiya Numako, Yannick Linard, Bruno Lanson, « On the nature of structural disorder in calcium silicate hydrates with a calcium/silicon ratio similar to tobermorite », *Cement and Concrete Research*, vol. 52, 2013, p. 31–37.

[GRO 86] G.W. Groves, P.J. Le Sueur, W. Sinclair, « Transmission electron microscopy and microanalytical studies of ion-beam-thinned sections of tricalcium silicate paste », *Journal of the American Ceramic Society*, vol. 69 , 1986, p. 353–356.

[HAM 81] S A. HAMID, « The crystal structure of the 11 Å natural tobermorite $Ca_{2.25}[Si_3O_{7.5}(OH)_{1.5}]\cdot 1H_2O$ », *Zeitschrift für Kristallographie*, vol. 154, 1981, p.189–198.

[HIL 52] R. HILL, « The Elastic Behaviour of a Crystalline Aggregate », *Proceedings of the Physical Society*, vol. 65, n° 5, 1952, p. 349-354.

[JEN 07] H.M. JENNINGS, J.J. THOMAS, J.S. GEVRENOV, G. CONSTANTINIDES, F.-J. ULM, « A multi-technique investigation of the nanoporosity of cement paste », *Cement and Concrete Research*, vol. 37, 2007, p. 329–336.

[JI 12] Q. JI, R.J.-M. PELLENQ, K.J.V. VLIETA, « Comparison of computational water models for simulation of calcium–silicate–hydrate », *Computational Materials Science*, vol. 1, n° 53, 2012, p.234-240.

[KAL 07] A.G. KALINICHEV, J. WANG, R. JAMES KIRKPATRICK, « Molecular dynamics modeling of the structure, dynamics and energetics of mineral–water interfaces: Application to cement materials », *Cement and Concrete Research*, vol. 3, n° 37, 2007, p. 337-347.

[KAM 09] S. KAMALI-BERNARD, F. BERNARD, « Effect of tensile cracking on diffusivity of mortar: 3D numerical modelling », *Computational Materials Science*, vol. 47, 2009, p.178–185.

[KIR 97] R.J. Kirkpatrick, J.L. Yarger, P.F. McMillan, Y. Ping, X. Cong, « Raman spectroscopy of C-S-H, tobermorite, and jennite », *Advanced Cement Based Materials*, vol. 5, 1997, p.93–99.

[KRE 96] Kresse G, Furthmüller J. « Efficient iterative schemes for ab initio total-energy calculations using a plane-wave basis set », *Physical Review B*, vol. 16, n° 54, 1996, p. 11169–11186.

[MAN 07] H. Manzano, J.S. Dolado, A. Guerrero, A. Ayuela, « Mechanical properties of crystalline calcium–silicate–hydrates: comparison with cementitious C-S-H gels », *Physica Status Solidi (a)*, vol. 204, 2007, p. 1775–1780.

[MER 01] S. MERLINO, E. BONACCORSI, T. ARMBRUSTER, « The real structure of tobermorite 11Å: normal and anomalous forms, OD character and polytypic modifications », *European Journal of Mineralogy*, vol.13, 2001, p. 577–590.

[MUR 10] S.J.MURRAY, V.J. SUBRAMANI, R. P.SELVAM, K. D. HALL, « Molecular Dynamics to Understand the Mechanical Behavior of Cement Paste », *Transportation Research Record: Journal of the Transportation Research Board*, n° 2142, 2010, p.75–82.

[PEL 08] R.J.-M. PELLENQ, NICOLAS LEQUEUX,HENRI VAN DAMME, « Engineering the bonding scheme in C-S-H: the iono-covalent framework », *Cement and Concrete Research*, vol. 2, n° 38, 2008, p. 159-74.

[PEL 09] R.J.-M. PELLENQ, AKIHIRO KUSHIMA, ROUZBEH SHAHSAVARI et al., « A realistic molecular model of cement hydrates », *Proceedings of the national academy of sciences of the united states of america*, vol. 38, n° 106, 2009,16102-16107.

[PLA 04] C. Plassard, E. Lesniewska, I. Pochard, A. Nonat, « Investigation of the surface structure and elastic properties of calcium silicate hydrates at the nanoscale », *Ultramicroscopy*, vol. 100 , 2004, p. 331–338.

[RIC 93] I.G. Richardson, G.W. Groves, « Microstructure and microanalysis of hardened ordinary Portland cement pastes», *Journal of Materials Science*, vol. 28, 1993, p. 265–277.

[SHA 09] R. SHAHSAVARI, M.J. BUEHLER, R.J.-M. PELLENQ, F-J.ULM, « First-Principles Study of Elastic Constants and Interlayer Interactions of Complex Hydrated Oxides: Case Study of Tobermorite and Jennite », *Journal of the American Ceramic Society*, vol.10, n°92, 2009, p.2323–2330.

[SHA 11] R. SHAHSAVARI, R.J-M. PELLENQ, F.J. ULM, « Empirical force fields for complex hydrated calcio-silicate layered material », *Physical Chemistry Chemical Physics*, vol.3, n° 13, 201, p.1002-1011.

[SCH 92] K-P. SCHRÖDER, J. SAUER, M.LESLIE, et al. « Bridging hydrodyl groups in zeolitic catalysts: a computer simulation of their structure, vibrational properties and acidity in protonated faujasites (H-Y zeolites) », *Chemical Physics Letters*, vol. 3-4, n° 188, 1992, p.320-325.

[TAY 56] H.F.W. TAYLOR, J. W. Howison, « Relationship between calcium silicates and clay minerals », *Clay Mineral Bulletin*, vol. 31, 1956, p.98–111.

[VAN 13] M. Vandamme, F.-J. Ulm, « Nanoindentation investigation of creep properties of calcium silicate hydrates », *Cement and Concrete Research*, vol. 52, 2013, p. 38 – 52.

[WU 07] Z.J. WU, E.J. ZHAO, H.P. XIANG, et al., « Crystal structures and elastic properties of superhard IrN2 and IrN3 from first principles », *Physical Review B*, vol.76, 2007, 054115.

[YU 99] P. Yu, R.J. Kirkpatrick, B. Poe, P.F. McMillan, X. Cong, « Structure of calcium silicate hydrate (C\S\H): near-, mid-, and far-infrared spectroscopy », *Journal of the American Ceramic Society*, vol. 82, 1999, p. 742–748.

[ZAO 12] A. ZAOUI, « Insight into elastic behavior of calcium silicate hydrated oxide (C–S–H) under pressure and composition effect », *Cement and Concrete Research*, vol. 2, n° 42, 2012, p.306-312.

[ZHA 05] W. ZHANG, H. WANG, J. Ye, « Structure and its variation of calcium silicate hydrates », *Journal of the Chinese Ceramic Society*, vol. 1, n° 33, 2005, p. 63–68. (in Chinese)